


Handbook
for
Generic Photonic IC Design

Editors: Meint Smit and Xaveer Leijtens

4-4-2026

 *Handbook for generic photonic IC design*, by the *Photonic Integration group*, Technische Universiteit Eindhoven, is licensed under a Creative Commons “Attribution-NonCommercial-NoDerivatives 4.0 International” license.

We traced the ownership of all figures used as far as we could. However, if you are a copyright owner and believe we used your work without permission, please contact us at coordinator@jeppix.eu.

Chapter 27

Polarization Based Components (draft)

JOS VAN DER TOL

Due to the planar nature of PICs their performance usually depends on the polarization of the guided wave. This can be problematic for applications in which the state of polarization is undefined, as e.g. within an optical fibre network. This chapter describes the solutions that are available to deal with this problem. However, polarization is not only a problem, it is also an extra degree of freedom in the use of optical waves. This has been recognized in optical communications, resulting in systems that use techniques like polarization multiplexing, alternating polarization transmission and polarization modulation. A number of integrated photonic circuits will be introduced in this chapter that can support such applications. The chapter will discuss the following subjects:

- Polarization independent devices
- Polarization splitters and combiners
- A TE generator
- Polarization manipulating circuit examples

27.1 Polarization independence

The two polarized modes, TE and TM, can behave very differently in a PIC. Their propagation constants are not the same, because of the boundary conditions on the edges of the waveguides. Also, the physical effects used to influence the modes can show a polarization dependence. This is e.g. the case for the electro-optic effects used to modulate the phase of the lightwave, such as the Pockels effect and the Kerr effect. Also the interaction with active material, to amplify, generate or detect light, can be polarization dependent.

As long as the optical circuit is operating on a specific and well defined polarized mode this is not a problem. If light is generated and processed on a PIC, for example in an optical transmitter, one can design all functions for a single polarization (usually TE). Although even in that case one has to be aware of possible polarization conversions, e.g.

polarization independence in tight bends, waveguide junctions or in certain taper structures. However, when light from the outside world with an undefined polarization state is coupled into the PIC it becomes important to design the circuits in such a way that a polarization independent response is obtained.

There are various methods to solve this problem. One could modify the waveguide for example, to equalize the propagation constants of TE and TM, so that their phase response is the same. Similar approaches are also possible to obtain polarization independence in the electro-optic response and the amplification of light. However, this leads to very specific solutions, not very suited for a generic integration platform, and is prone to tight tolerances. Here we will discuss two approaches which do not have these disadvantages, by using the tolerant devices introduced in Chapter 11.

polarization diversity The first method is called polarization diversity. It is based on the use of a polarization splitter. After separating the TE- and TM-polarized modes with this device each of them is processed independently in parallel circuits. If required the two can be combined again in a single waveguide with a polarization combiner, which is just the polarization splitter used in the reverse direction. We will also introduce a second method for polarization independence, which uses averaging of the responses for the TE- and the TM-modes.

27.2 Polarization diversity

Central to the polarization diversity approach is the polarization splitter (PS), which is a composite building block in itself. Therefore we will introduce this function first.

27.2.1 Polarization splitter/combiner¹






There are many ideas proposed in the literature for polarization splitters. Not all of these are suitable for generic integration. We will concentrate on a few that do.

polarization splitter Polarization splitters that can be integrated with other functions on a chip are crucial in an integration technology with polarization handling capability. As the name implies, polarization splitters separate the TE and TM modes at the input and route them to different outputs. As these are usually reciprocal devices, they can also be used reversely, as polarization combiners. Passive polarization splitting is preferred over active splitting to minimize power consumption and to avoid the need for tuning. For passive splitting, birefringence is required to obtain a difference in propagation for TE and TM polarized light. The birefringence needed for splitting can be obtained in a number of ways. It can be by loading a waveguide with metal [392][393]; by using the modal birefringence of the fundamental mode (demonstrated in InP [394][395] and Si [396][397]) or the higher-order TE and TM modes [398][399]; or by using waveguides with a different geometry for the different polarizations [400][401]. The most promising devices suited for integration in InP are shown in Table 27.1.

mode-evolution interference As can be seen from the table, the splitting can be obtained by using different principles: splitting based on mode-evolution in an adiabatic coupler (splitter A) [398], which results in tolerant, but very long devices; or splitting based on interference. The splitters based on the latter principle (B–E) can be divided in two categories: devices that use metal loading of the waveguides to achieve birefringence (B, C) and devices that employ modal birefringence and consist solely of waveguides (D, E) that can be

¹This section is based on the PhD Thesis of Luc Augustin, section 5.1. [161]

Table 27.1: Different passive polarization splitters

Ref.	Principle	Schematic	Fabrication	Performance
A [83]	Mode evolution. Modal birefringence of the first-order mode (only 1×2)		Single shallow RIE etch	<ul style="list-style-type: none"> • L=6000 μm • $\text{SR}_{\text{TE}}=12.0$ dB • $\text{SR}_{\text{TM}}=13.1$ dB • Loss < 1 dB
B [77]	Interference: directional coupler employing birefringence obtained by strip-loading one waveguide with metal (2×2)		Au sputtered metal patch, RIE etched shallow waveguides.	<ul style="list-style-type: none"> • L=1600 μm • $\text{SR}_{\text{TE}}=12.2$ dB • $\text{SR}_{\text{TM}}=30$ dB • Loss 0.3 dB
C [78]	Interference: Mach-Zehnder Interferometer employing birefringence obtained by strip-loading one waveguide with metal (2×2)		Au sputtered metal patch, RIE etched shallow waveguides.	<ul style="list-style-type: none"> • L=3300 μm • $\text{SR}_{\text{TE}}=16$ dB • $\text{SR}_{\text{TM}}=13$ dB • Loss 1.5 dB
D [80]	Interference: directional coupler employing modal birefringence of the fundamental system modes (1×2 demonstrated, 2×2 is possible)		2 step selective wet etch.	<ul style="list-style-type: none"> • L=3900 μm • $\text{SR}_{\text{TE}}=16$ dB • $\text{SR}_{\text{TM}}=17$ dB • Loss < 1.5 dB
E [84]	Interference: directional coupler employing modal birefringence of first-order modes (1×2)		Single shallow RIE etch.	<ul style="list-style-type: none"> • L=1100 μm • $\text{SR}_{\text{TE}}=13$ dB • $\text{SR}_{\text{TM}}=20$ dB • Loss < 1 dB

etched in a single step. The latter are advantageous over the ones with metal on top, because of the relaxed processing. They have the advantage to be short, have a low loss and a high splitting ratio. A drawback are the very stringent fabrication tolerances. The device employing the birefringence of the fundamental mode (D) has to meet even tighter conditions, as in this case, for both TE and TM, a strict coupling condition has to be met: TE has to couple through and TM requires exactly half that coupling length to couple through and back again. In the device that uses the modal birefringence of the higher-order modes (E [399]), only one condition has to be met: TE has to couple. This makes the latter device more tolerant and shorter. Even shorter splitters based on photonic crystal waveguides [402] are reported, but these have the disadvantage of higher losses and more complex processing, making them difficult to integrate. This makes splitters based on interference the most suitable for the integration with active and passive components. In this section two types of polarization splitters based on interference are described. The principle, design, fabrication and results are discussed. First a tolerant 1×2 directional coupler based PS is reported. This device has a high splitting ratio, but is relatively long and therefore more difficult to integrate. Next a splitter based on a Mach Zehnder Interferometer with polarization converters is presented. This device is short and is fully integrable in the standard active-passive integration scheme.

27.2.2 Directional coupler polarization splitter²

As stated before, splitters based on modal birefringence have very stringent fabrication tolerances. It can be realized as a directional coupler, introduced in chapter 20. Examples are given in Table 27.1 (B, D and E), but without any measures to alleviate the tolerance problem. Tapering both the waveguides and the coupling region increases the tolerances in directional couplers at the cost of a somewhat increased length [403]. This section will describe a polarization splitter based on modal birefringence with tapered waveguides in combination with a tapered coupling region that has an increased tolerance in fabrication.

To use the directional coupler as a polarization splitter, a polarization-dependent coupling is required. The splitting is based on modal birefringence of the higher-order modes: their propagation constants differ significantly for different polarizations; much more than for the fundamental modes. The splitter consists of an asymmetric directional coupler with a narrow and a wide waveguide (Fig. 27.1). The widths are chosen such that the propagation constant of the fundamental mode in the narrow waveguide equals the propagation constant of a higher-order mode in the wide waveguide for one polarization only. Fig. 27.2 shows the calculated mode intensity profiles. It is seen that for TE the fundamental and third-order waveguide modes are resonant, but for TM this is not the case. Only the resonant polarization can couple. Over a distance equal to the coupling length, the light in this polarization is fully transferred from the narrow to the wide waveguide. The same principle is repeated to couple from the wide waveguide to the narrow TE-output waveguide. In this way the third-order mode is converted back to the fundamental mode and a double filtering is achieved. The TM output has to bend away from the wide waveguide to prevent the TE-polarized light to couple back into it.

The resonant modes are determined by calculating the propagation constant as a function of the width at a wavelength of 1555 nm, using the effective index method (Fig. 27.4) for a waveguide cross section as shown in Fig. 27.3. This cross section is fully

²This section has been partially copied from the PhD Thesis from Luc Augustin [161], section 5.2.

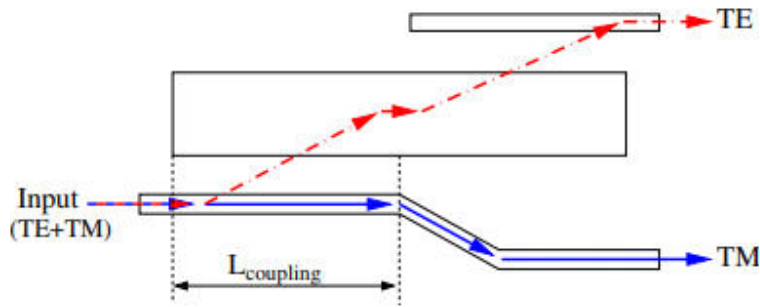


Figure 27.1: Principle of the polarization splitter.

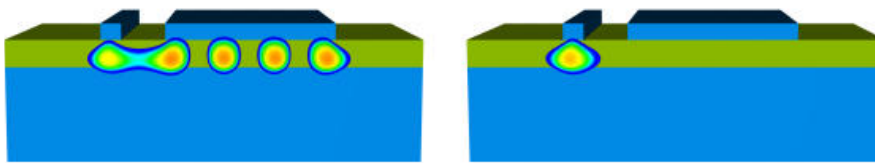


Figure 27.2: Resonant TE-mode (left) and non-resonant TM-mode for (right).

compatible with the layer stack and processing for the generic integration platform. The propagation constants match for TE_{00} and TE_{03} for widths of $0.8\mu\text{m}$ and $6.9\mu\text{m}$ respectively. Furthermore, for a width of $6.9\mu\text{m}$ no TM mode is resonant with the fundamental mode for the narrow waveguide. In fabrication, the width of the waveguides can deviate from the designed width, which causes a change in the propagation constants and thereby destroys the resonance of the modes. This leads to a reduced coupling for one polarization and a possibly increased coupling for the other, which will deteriorate the splitting ratio of the device. To compensate for these errors in fabrication, the wide waveguide is tapered as is shown in Fig. 27.5. The tapering is possible because from Fig. 27.4 it can be seen that the propagation constants for higher-order TM modes do not match the propagation constant in the narrow waveguide in a width range of more than 750 nm . This large range yields a window for tapering, while preserving the mismatch for TM.

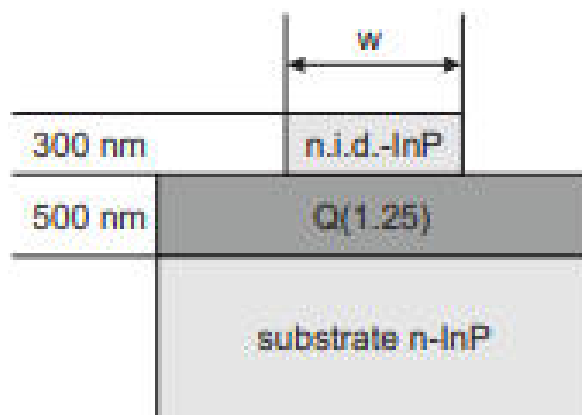


Figure 27.3: Cross section.

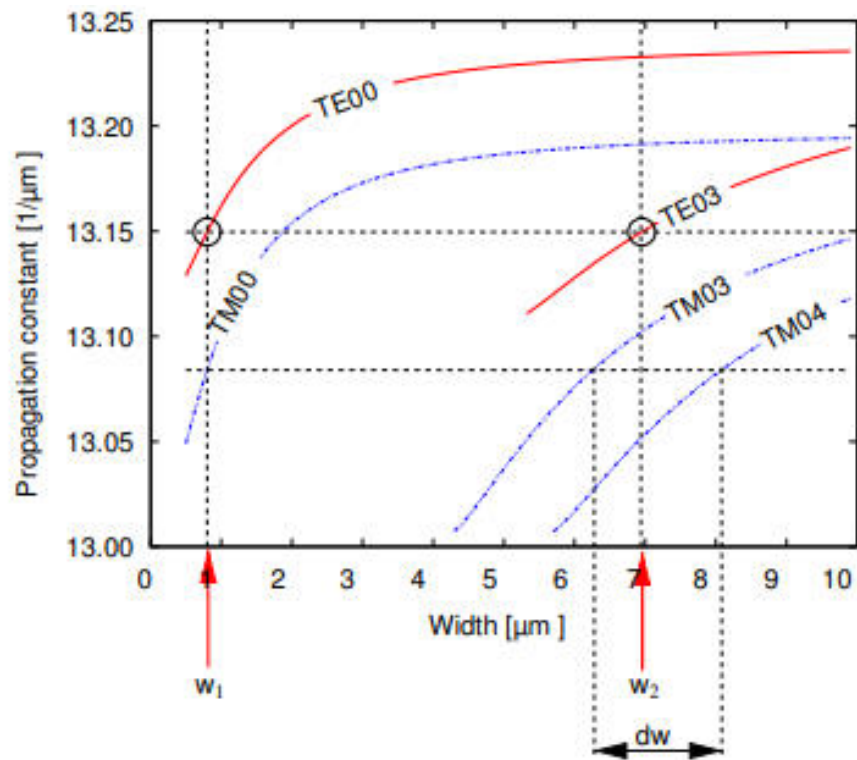


Figure 27.4: Propagation constants as a function of width for the relevant modes. w_1 (w_2) is the width of the narrow (wide) waveguide. The horizontal lines indicate matching propagation constants for TE_{00} and TE_{03} , but not for TM_{00} and any other mode. dw is the range over which there is no matching for TM_{00} .

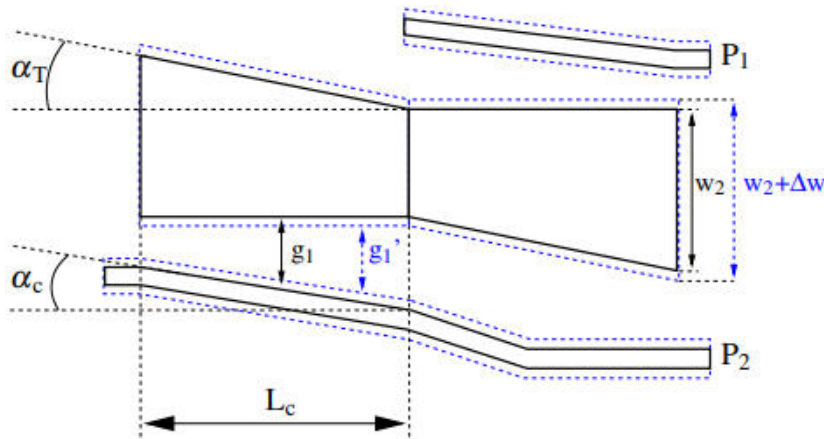


Figure 27.5: Schematic of the polarization splitter. Note that the vertical dimensions are enlarged for clarity, the dashed lines visualize the broadening of the waveguides that can be introduced in fabrication..

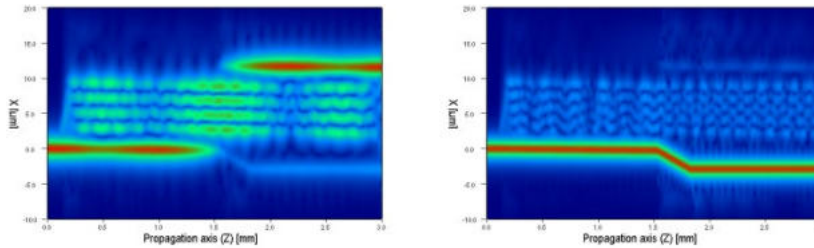


Figure 27.6: Top view of the propagated field in the polarization splitter for TE (left) and TM (right)..

The design strategy for tapering is explained in detail in [161], and will not be repeated here. The basic ideas are:

1. Along the taper there is a point where the resonant modes exist (for TE), within *taper* the tolerance range required.
2. For the other polarization (here TM) no such point is present.
3. The taper angle is chosen to provide an effective area around the resonance point to match one coupling length. Larger angles lead to under coupling, smaller to over coupling. With simulations the right angle can be found. *taper angle*
4. In order to improve the tolerance even further, the gap between the waveguides is also tapered. If this is done properly, this gap is the same for any resonance point at any width deviation.

The propagation of the TE and the TM modes is shown in fig. 6.

The simulated and the experimental results for the splitting are given in fig. 27.7. From the figure it is clear that the measured devices show an SR larger than 13 dB for a large width range. For TM polarized light, the splitter is good for a width range of at least 150 nm. For TE the range is limited to approximately 100 nm. Two maxima are present in the TE results, as is also seen from simulations. The best splitter (40 nm wider) has

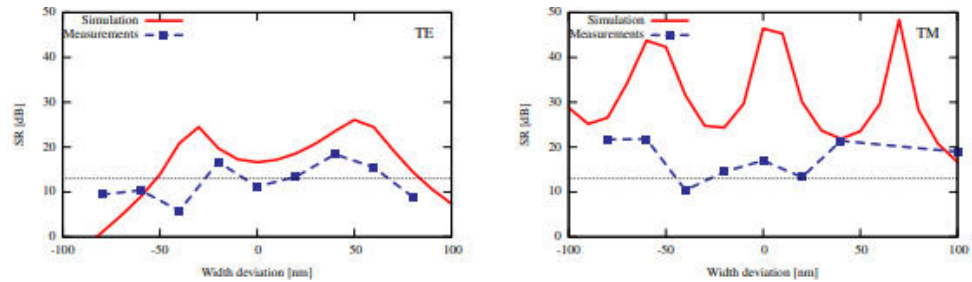


Figure 27.7: Splitting ratio measurements at 1560 nm, compared to BPM simulations for TE (left) and TM (right) polarization, the dotted line indicates 13 dB splitting ratio..

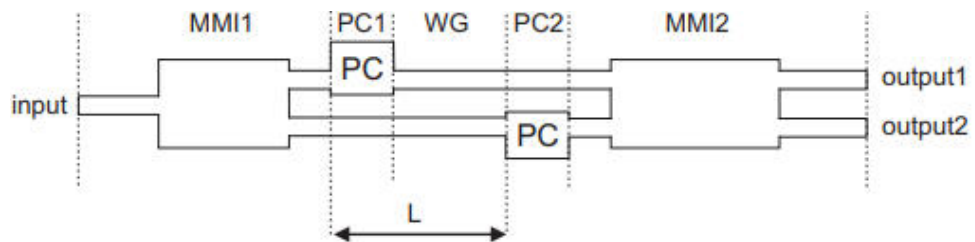


Figure 27.8: Schematic of the MZI polarization splitter/converter..

an SR of 18 dB for TE and 20 dB for TM, better than any of the devices in Table 27.1. The overall performance as shown in Fig. 27.7 is less than predicted by simulations, most probably caused by scattering from rough waveguide walls, which can lead to unwanted coupling. Because of this, the local minimum for TE at 0 nm deviation is slightly lower than 13 dB.

27.2.3 MZI Polarization splitter³

The polarization splitters described in the previous section have the advantage of low loss and high splitting ratios. A drawback is their length (1 to 3 mm) which is large compared to other components on the chip. Furthermore, the devices have to be critically defined at a deeper etching level than most of the active and passive devices, which poses another problem. A new design is investigated that solves these problems. This is a compact, 600 μm long, integrated splitter based on polarization converters (PCs). It consists solely of passive waveguides and PCs and is thus the device of choice for a generic integration platform in which a polarization converter can be integrated as described in Chapter 11.

Mach Zehnder Interferometer

The device consists of a Mach Zehnder Interferometer with polarization converters in both arms, as is depicted in Fig. 27.8. Light coupled into the input waveguide of the first Multi-Mode Interference coupler (MMI) is split into the two branches with equal power and phase. In the upper branch a polarization converter is placed that rotates the polarization over 90°, so after this, the orthogonal polarization propagates through this branch. In the lower branch the light in the original polarization propagates over a distance L before being rotated in a polarization converter. The birefringence in the waveguides causes a phase shift between light in the arms. This phase shift is equal in magnitude but opposite in sign for TE and TM. When both signals are combined in

³This section has been partially copied from the PhD Thesis from Luc Augustin [161], section 5.3.

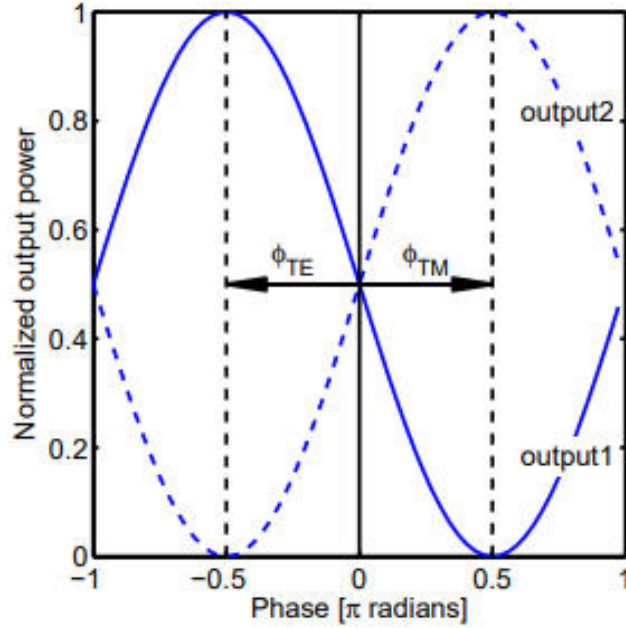


Figure 27.9: MZI polarization splitter principle. The phase shift between the two branches determines the output port distribution. Due to the positioning of the PCs TE and TM input signals have opposite phase shifts, which couples them to different output ports if the phase shift is + and $-\pi/2$ rad.

the output MMI, the phase difference causes one polarization to appear in one output while the opposite polarization goes to the other output (see Fig. 27.9). To achieve the desired splitting, the phase difference between the branches needs to be $\pi/2$ radians. This is obtained when:

$$L = \frac{\pi}{2}(\beta_{TE} - \beta_{TM}), \quad (27.1)$$

where $\beta_{TE, TM}$ are the propagation constants for both polarizations.

The performance of the MZI-PS can be simulated using transfer matrices to describe each part of the circuit (see [161]). It can be quantified in terms of the Splitting Ratio (SR) of the splitter, defined as the total power in the desired port (output1 for TE input) *splitting ratio* divided by the total power in the undesired port:

$$SR(TE_{in}) = 10 \log\{(P_{TM, out1} + P_{TE, out1}) / (P_{TM, out2} + P_{TE, out2})\} \quad (27.2)$$

For a splitting ratio larger than 13 dB, a conversion c_{PC} above 90% is needed. The net *conversion* circuit conversion c_{PS} is the conversion of the whole polarization splitter circuit, this is the conversion obtained at the desired output port (output1 for TE input):

$$c_{PS}(TE_{in}) = P_{TM, out1} / (P_{TE, out1} + P_{TM, out1}) \quad (27.3)$$

Figure 27.10 shows the splitting ratio and the net circuit conversion as a function of the conversion of the PCs in the arms.

The c_{PS} is larger than 95%, for c_{PC} above 90%, because the unconverted part is split equally over the outputs. It can be seen that for a SR of better than 20 dB a conversion

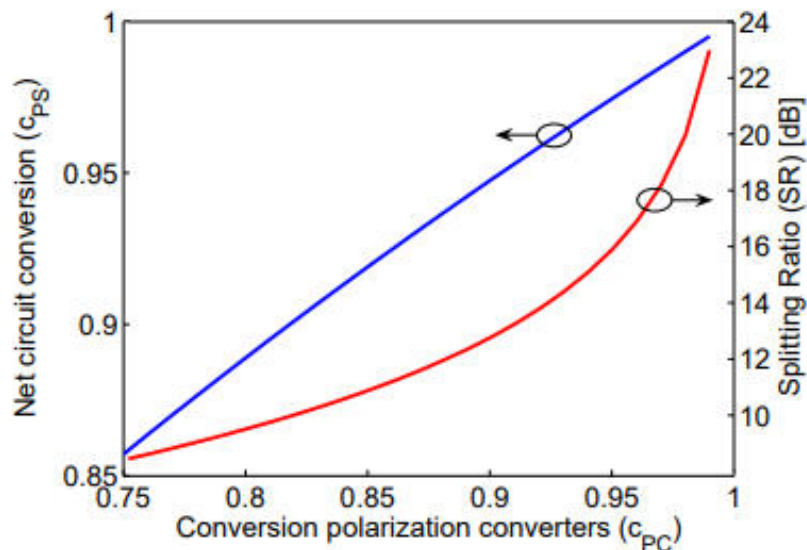


Figure 27.10: Circuit polarization conversion and splitting as a function of the PC-performance..

of 98% is needed for the PCs in the MZI-branches. From Chapter 11 it can be seen that such a value is easily achievable with a double-section PC.

Of course also other parameters in the circuit of Fig. 27.8 have to be controlled, like the length L and the performance of the MMI-couplers. A special requirement for MMI2 (the 2x2 coupler at the output) is that it should be a polarization independent device. This is generally the case with a generic integration platform.

This PS has so far only been realized once, in 2008 (ref. [161]). The conversion of the PCs was limited then to 87%, resulting in a splitting ratio of around 10 dB. In view of the improvements obtained in polarization converters since then (see Chapter 11) it is straightforward to achieve better performances.

27.2.4 TE-generator⁴

The planar geometry of InP waveguides introduces challenges related to the polarization of the guided light. In particular, the waveguide's birefringent nature causes transverse electric (TE) and transverse magnetic (TM) modes to propagate differently. This polarization-dependent behaviour means that most photonic components are designed to operate best for a single polarization, typically the TE mode, due to its lower propagation loss, better confinement, and higher optical gain in active quantum well materials [404]. Consequently, the performance for the orthogonal TM mode is often suboptimal. This becomes problematic in applications like fibre-optic communication, where the input light typically has an undefined polarization state. When such light passes through a polarization-sensitive PIC, the device performance varies strongly with the state of polarization, posing a severe problem for the system [405]. It is therefore a useful function to transform any state of polarization into a pure TE mode to ensure compatibility and best performance of subsequent integrated functions. Conventional approaches of polarization diversity involve the use of a polarization beam splitter (PBS) to separate the input light into two orthogonal states (TE

*polarization beam
splitter*

⁴This section is based on a paper submitted by Kolsoom Mehrabi to Optics Letters.

and TM). One of these beams (e.g., TM) can then be converted into the other polarization (TE) using a polarization rotator [406]. While conceptually straightforward, this method faces practical limitations. It leads to extra insertion losses and reflections due to the use of multiple optical components, reducing system efficiency. The need for separate components also results in a large footprint. Additionally, the bandwidth is often restricted by the narrow operating range of the integrated polarization beam splitters, making the approach less suitable for high-speed or broadband applications [53].

Here an alternative approach is given: a passive device that can convert any arbitrary polarization state into a pure TE signal. This functionality will be referred to as the "TE generator building block." It provides a compact and simple mechanism and can be used in various applications such as polarization controllers and scramblers, and in general for all polarization diversity circuits.

TE generator

Principle of operation

The proposed functionality requires converting the TM component of the incoming signal into a TE mode while maintaining the TE component. However, the reciprocal nature of the polarization conversion prevents this from being achieved using a standard polarization converter (PC). To circumvent this problem, we utilize waveguide birefringence, where TE and TM modes accumulate different phase shifts during propagation. The designed waveguide section for this supports the first two orders of both TE and TM modes, allowing for the selective manipulation of their relative phases. We refer to this as a bimodal phase-shifting section, which is engineered such that the phase shift between the TE₀₀ and TM₀₁ modes (which are created from a TE input signal with two 50% polarization converters) is an odd multiple of π , while the phase shift between the TM₀₀ and TE₀₁ modes (similarly created from a TM-input) is an even multiple of π . This is the basis for achieving the desired polarization transformation. The proposed building block incorporates two pairs of 50% polarization converters, distributed over two branches and each with a different rotation direction for the mode in each branch, and the specifically designed bimodal phase shifter section described above. As illustrated in Fig. 27.11(a), passing through the 50% polarization converter results in a $\pi/2$ phase difference between the converted signal and the input signal, while the non-converted component remains unchanged in both phase and polarization.

bimodal phase shifting

The operation of the polarization transformer building block for TE injected signals is shown in Figs. 27.11(b).

The input power is equally divided between two branches after the 1x2 MMI and passes through 50% polarization rotators, applying $\pi/2$ rotation on the Poincaré sphere for the input signal. If we split the resulting signal into the TE and TM modes, the TM signal of the upper branch has $\pi/2$ radians phase, while the TM part of the signal in the lower branch has $-\pi/2$ radians phase, because of the opposite rotation direction of the converters. These signals are directed into a bimodal phase-shifting section designed to support the propagation of the two lowest-order modes of both polarizations, i.e., TE₀₀, TM₀₀, TE₀₁, and TM₀₁ modes (where the second subscript denotes the in-plane direction of the chip). The TE₀₀ mode with phase zero excites the TE₀₀ mode of the bimodal phase shifter section. The TM₀₀ mode with phase $\pi/2$ and the TM₀₀ mode in the other branch with phase $-\pi/2$ radians excite the TM₀₁ mode in the bimodal section. For a TE-input, the TM-part of the light exits the bimodal phase shifter with the opposite relative phase as it had after the first 50% PC-pair. This means that the

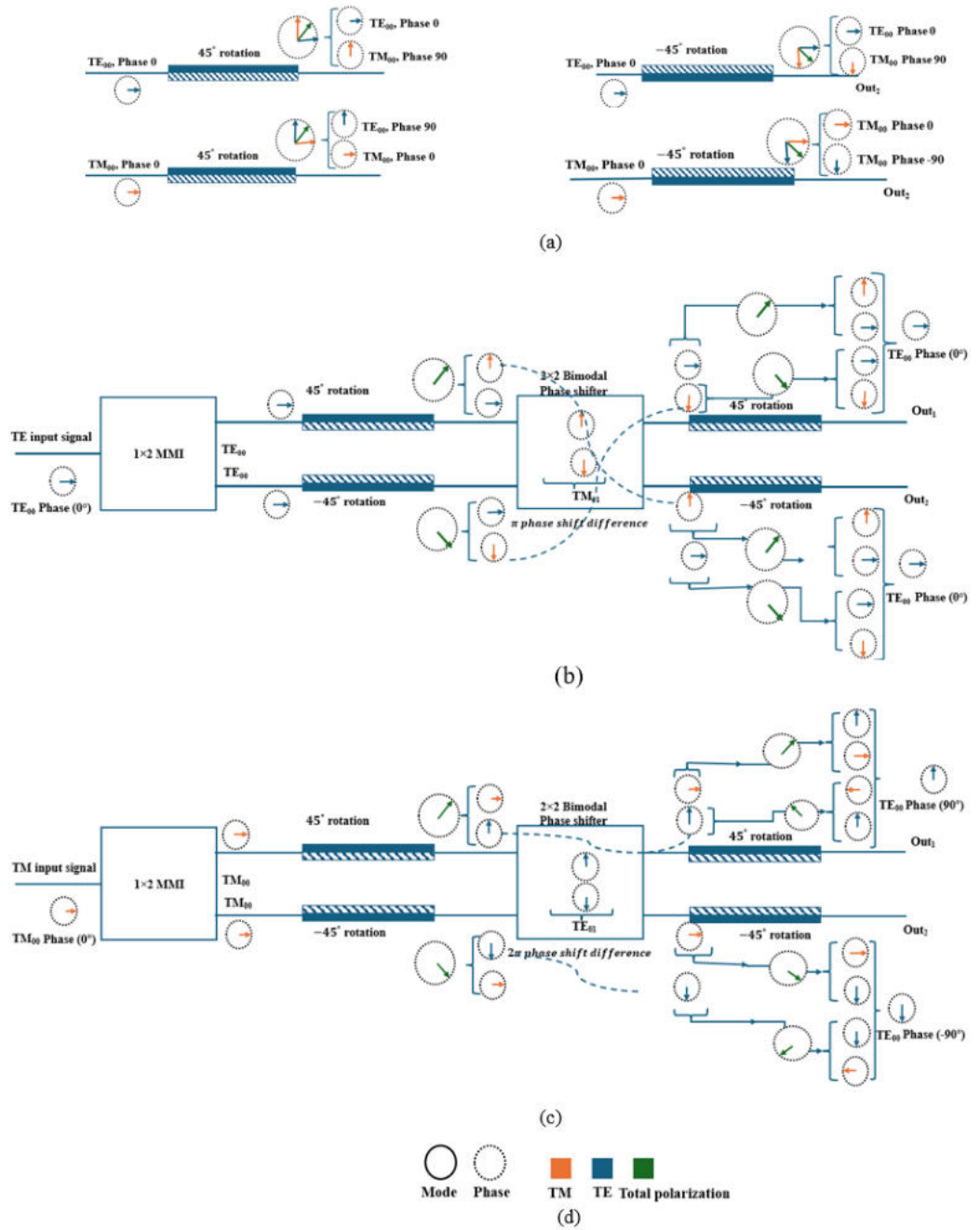


Figure 27.11: Description of the proposed building block behaviour. (a) Explanation of how light passes through the 50% polarization converter. (b) the TE-injected signal and (c) the TM-input signal. (d) Schematic explanation: The blue/orange arrows in the solid circles indicate the TE/TM modes, while the blue/orange dashed circles and arrows represent the TE/TM mode phases. Green arrows in the dashed circle indicate the total polarization states after ±45° rotation, which are subsequently decomposed into TE and TM components..

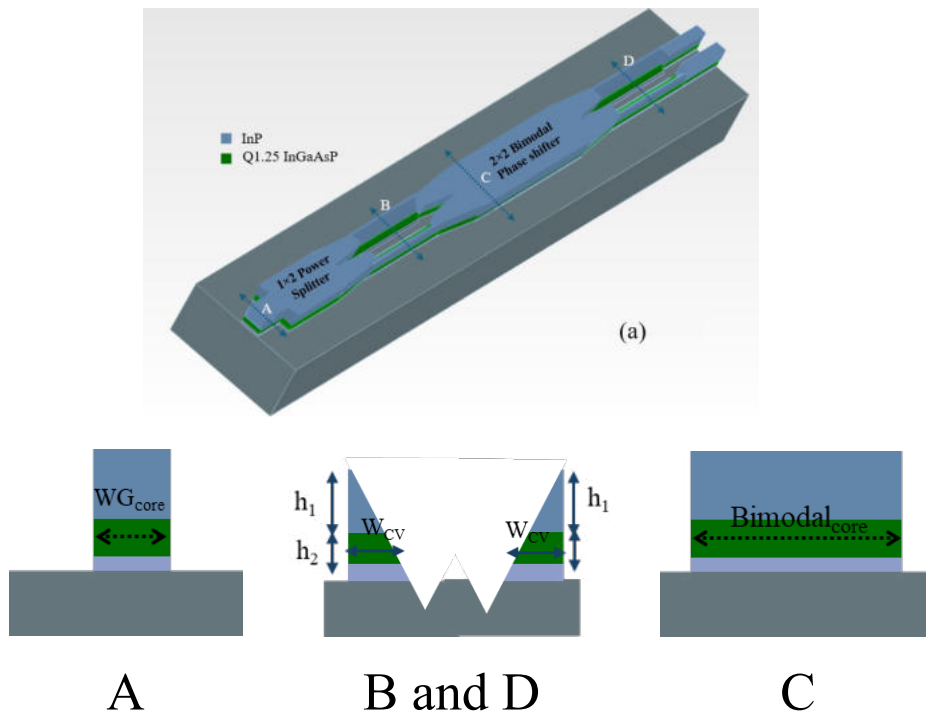


Figure 27.12: TE generator building block (a). Three-dimensional schematic (b) Schematic cross-section of the device at different points (A, B, C, and D) along the device length..

conversion in the second pair is inverted, so the total conversion cancels out and all light ends up in the TE-mode.

Fig. 27.11(c) shows how the building block works when a TM signal is injected into the input. The behaviour is the same as for the TE mode injection, with one difference at the input of the bimodal section. In this case, the TM signals appear with the same phase, exciting the TM_{00} mode of the bimodal section, while the TE_{00} modes at the inputs appear with opposite phases and excite the TE_{01} mode of the bimodal section. The bimodal phase shifter applies a 2π phase shift between the TM_{00} and TE_{01} modes. Therefore the converted TE-part enters the second PC-pair with the same relative phase as it had from the first pair, so that the two conversions add up to a full conversion into the TE-mode.

The three-dimensional configuration of the proposed building block is illustrated in Fig. 27.12. In this figure, WG_{core} represents the waveguide core width, and the core of the polarization converter is shown as W_{cv} . The width of the phase shifter section is labelled as $Bimodal_{core}$. A linear taper is designed to ensure low-loss and mode-preserving coupling between the waveguides and the bimodal phase shifter. The total building block length, including the input and output waveguides, is only $281 \mu m$, and the width is $4.12 \mu m$, highlighting the compact footprint of the design and its suitability for dense photonic integration.

Theory

The system is modelled using a transfer matrix method, where each circuit section is represented by a matrix operating on vectors corresponding to the complex amplitudes of the involved modes. The system considers four amplitude components: TE and TM modes in the upper and the lower arms, and the four modes in the bimodal phase-shifting section. The input vector is represented by a combination of TE and TM modes with normalized amplitude and phase for the TE mode (amplitude 1, phase 0). This results in:

$$V_{\text{in}} = \begin{pmatrix} A_{\text{TE}} \\ 0 \\ A_{\text{TM}} \\ 0 \end{pmatrix} = \begin{pmatrix} 1 \\ 0 \\ ae^{j\varphi} \\ 0 \end{pmatrix} \quad (27.4)$$

The zero values indicate that there is only one input port, designated here as the “upper” arm.

The power splitter matrix, M_{split} , couples the input modes to the upper and lower branches, with a normalization factor of $1/\sqrt{2}$, ensuring power conservation:

$$M_{\text{split}} = \frac{1}{\sqrt{2}} \begin{pmatrix} 1 & 0 & 0 & 0 \\ 1 & 0 & 0 & 0 \\ 0 & 0 & 1 & 0 \\ 0 & 0 & 1 & 0 \end{pmatrix} \quad (27.5)$$

Next, the two 50% polarization converters are applied. Here we considered conversion efficiency as c to include fabrication and design error effects. Each converter has a phase shift of 90° between the original and converted modes, modelled by the matrix

$$M_{\text{PC1}} = \frac{1}{\sqrt{2}} \begin{pmatrix} \sqrt{1-c} & 0 & j\sqrt{c} & 0 \\ 0 & \sqrt{1-c} & 0 & -j\sqrt{c} \\ j\sqrt{c} & 0 & \sqrt{1-c} & 0 \\ 0 & -j\sqrt{c} & 0 & \sqrt{1-c} \end{pmatrix} \quad (27.6)$$

The “ j ” and “ $-j$ ” indicate the opposite rotation of the conversion in the two arms. This is obtained by making the converters mirror images of each other.

The fields from the polarization converters are then combined into the bimodal phase-shifter section, where the modes are defined as TE_{00} , TE_{01} , TM_{00} , and TM_{01} . The connection matrix describes the coupling into these modes:

$$M_{\text{Conn1}} = \frac{1}{\sqrt{2}} \begin{pmatrix} 1 & 1 & 0 & 0 \\ 1 & -1 & 0 & 0 \\ 0 & 0 & 1 & 1 \\ 0 & 0 & 1 & -1 \end{pmatrix} \quad (27.7)$$

The bimodal phase-shifting section introduces phase shifts between the modes: a π radians shift between TE_{00} and TM_{01} and a 2π radians shift between TM_{00} and TE_{01} ,

represented by the matrix M_{Bimod} . To consider the fabrication errors, a phase shift error of $\Delta\varphi_1$ and $\Delta\varphi_2$ are introduced for TE and TM modes, respectively.

$$M_{\text{Bimod}} = \frac{1}{\sqrt{2}} \begin{pmatrix} 1 & 0 & 0 & 0 \\ 0 & 1 & 0 & 0 \\ 0 & 0 & e^{j\Delta\varphi_1} & 0 \\ 0 & 0 & 0 & -e^{j\Delta\varphi_2} \end{pmatrix} \quad (27.8)$$

The connection to arms with the second pair of polarization converters is modelled by M_{Conn2} , which is identical to M_{Conn1} , and the second polarization converter section is identical to the first, so $M_{\text{PC2}} = M_{\text{PC1}}$.

Finally, the total operation of the system is described by the multiplication of these matrices:

$$V_{\text{out}} = M_{\text{PC2}} M_{\text{Conn2}} M_{\text{Bimod}} M_{\text{Conn1}} M_{\text{PC1}} M_{\text{split}} V_{\text{in}} \quad (27.9)$$

When a TE input is applied, the two output ports generate in-phase signals, whereas a TM input leads to out-of-phase signals. This distinction ensures the preservation of reciprocity, as the TE and TM inputs couple into different system modes at the output.

Upon evaluating the matrices, the output powers for TE and TM inputs are:

$$P_{\text{out}} = V_{\text{out}} \times V_{\text{out}}^* \quad (27.10)$$

$$P_{\text{out,TE}} = \begin{pmatrix} \text{TE-TE (port1)} \\ \text{TE-TE (port2)} \\ \text{TE-TM (port1)} \\ \text{TE-TM (port2)} \end{pmatrix} = \frac{1}{8} \begin{pmatrix} 4c^2 + 4(1-c)^2 + 8c(1-c) \cos(\Delta\varphi_2) \\ 4c^2 + 4(1-c)^2 + 8c(1-c) \cos(\Delta\varphi_2) \\ 4c(1-c)\{2 + 2 \cos(\Delta\varphi_2)\} \\ 4c(1-c)\{2 + 2 \cos(\Delta\varphi_2)\} \end{pmatrix} \quad (27.11)$$

$$P_{\text{out,TM}} = \begin{pmatrix} \text{TM-TE (port1)} \\ \text{TM-TE (port2)} \\ \text{TM-TM (port1)} \\ \text{TM-TM (port2)} \end{pmatrix} = \frac{1}{8} \begin{pmatrix} 4c(1-c)\{2 + 2 \cos(\Delta\varphi_1)\} \\ 4c(1-c)\{2 + 2 \cos(\Delta\varphi_1)\} \\ 4c^2 + 4(1-c)^2 - 8c(1-c) \cos(\Delta\varphi_1) \\ 4c^2 + 4(1-c)^2 - 8c(1-c) \cos(\Delta\varphi_1) \end{pmatrix} \quad (27.12)$$

For $c = 0.5$ and $\Delta\varphi_1 = \Delta\varphi_2 = 0$ the output contains only TE-light in the output ports.

TE generator building block design

For the operation of the device, an odd multiple of π rad phase shift between the TE_{00} and TM_{01} modes, and an even multiple of π rad phase shift between TM_{00} and TE_{01} modes, is targeted. In our design, the width and length of the bimodal phase shifter section are chosen such that it results in 3π phase difference between TE_{00} and TM_{01} , and 2π phase difference between TM_{00} and TE_{01} . Based on simulation data the width of the bimodal MMI section is chosen as $4.12 \mu\text{m}$, while the length is $63 \mu\text{m}$. The length of the PCs is set to $66.7 \mu\text{m}$.

Figure 27.13 indicates the propagation of the modes through the device when TM polarized light is injected. In figure 27.13(a), the polarization of light at both outputs is

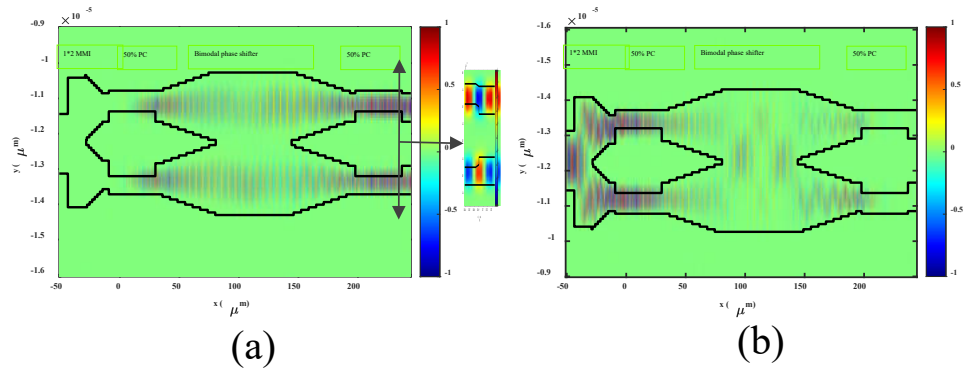


Figure 27.13: TM injection simulation results (a) The y- component of electric field (TE), (b) The z-component of electric field (TM)..

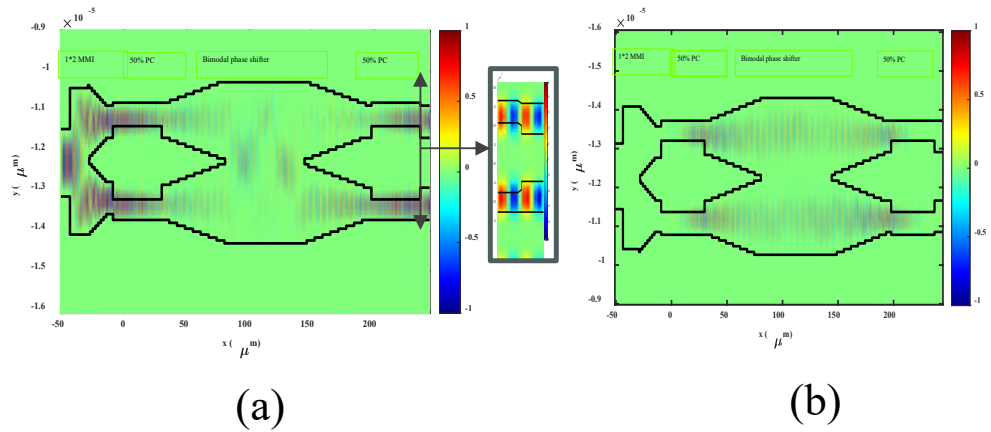


Figure 27.14: TE injection simulation results (a) The y-component of electric field (TE), (b) The z-component of electric field (TM)..

TE; however, they are out of phase because they are generated by mirrored polarization converters. The simulated loss is lower than 1 dB. The response of the device to TE input light is depicted in Fig. 27.14. By controlling the phase change in the bimodal section, the converted TM light cancels out, allowing only TE light to appear at the output. As depicted in Fig. 27.14(a), the output signals are in phase.

Characterization of realized device.

The TE-generator has been realized using a combination of wet- and dry-etching techniques. Figure 27.15 shows SEM-pictures of the result.

The fabricated polarization converter/splitter was characterized (see Fig. 27.16). The TE fraction at the output varies from 92% to 53% for a TE input and from 66% to 98% for a TM input across the measured wavelength range. These results confirm the functionality of the device as a potentially robust polarization transformer. Conversion efficiency of the device based on measurement data is calculated in Fig. 27.17. The fitting function is defined using Eqs. 27.11 and 27.12, where the conversion efficiency c is considered as a constant, and the wavelength dependence is incorporated into $\Delta\varphi_1$ and $\Delta\varphi_2$. Based on the fitting function, the polarization converters operate efficiently,

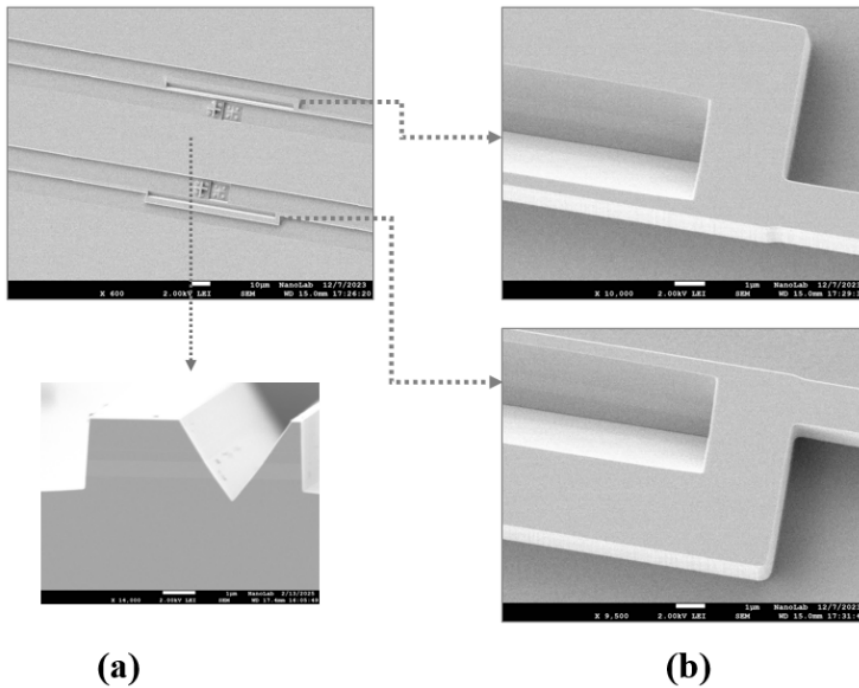


Figure 27.15: Scanning electron microscope (SEM) image of the fabricated device after wet etching (a) cross-section view, (b) top view..

achieving a 49% conversion rate, which closely matches the designed value of 50%. However, phase errors of -1.4 rad ($\Delta\varphi_1$) for the TE input and $+0.3$ rad ($\Delta\varphi_2$) for the TM input are observed in the bimodal section at the reference wavelength of 1.55 μm . The TE generating device that has the correct polarization converter width (1.425 μm) on the wafer happens to have a bimodal section length of 46.5 μm . This is because of parameter variations in the circuits designed on the chip. Despite this deviation, the realized device demonstrates promising polarization conversion. At 1.526 μm , the TE output reaches 84% for both TE and TM inputs, ensuring reliable operation for arbitrary polarization states. To evaluate the device performance in the absence of phase errors, the conversion efficiency was calculated by setting the TE and TM input phase errors to zero. Figure 27.18 presents the resulting device performance, where the conversion efficiency spectrum becomes symmetric and the maximum is shifted to the centre of the wavelength range. As can be seen, correcting the phase error results in an efficiency of $>99\%$ and a broad wavelength range of >50 nm.

It should be noted that the bimodal phase shifter can also be designed to convert to TM-output modes, if desired. Overall, the results confirm the device's effectiveness for polarization management in photonic integrated networks.

27.3 Some polarization manipulating circuit examples

In this section we will present some circuits on the InP generic integration platform, that use polarization splitters and converters to obtain various polarization related functions.

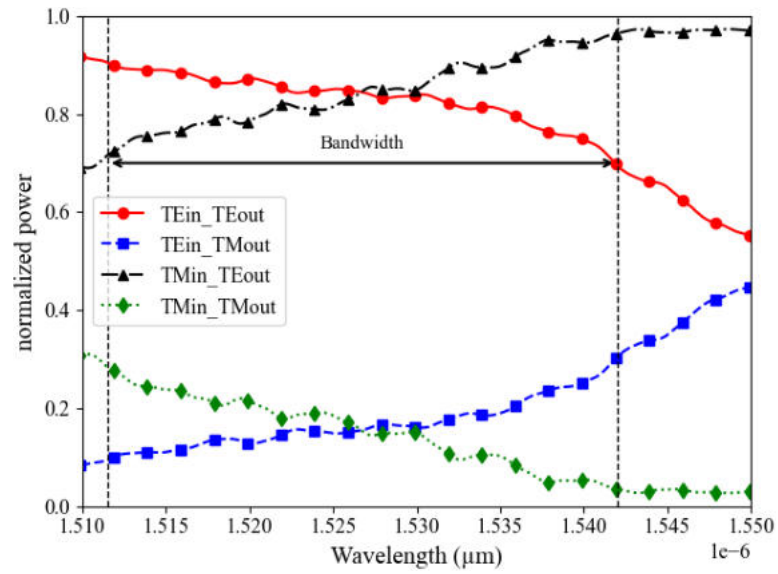


Figure 27.16: Normalized output power spectra showing TE/TM fractions from the two outputs of the TE generator building block for a converter length of 66.7 μm, widths of 1.425 μm, and a bimodal section length of 46.5 μm. Red/blue: TE input; black/green: TM input. The operational bandwidth is indicated between the vertical dashed lines..

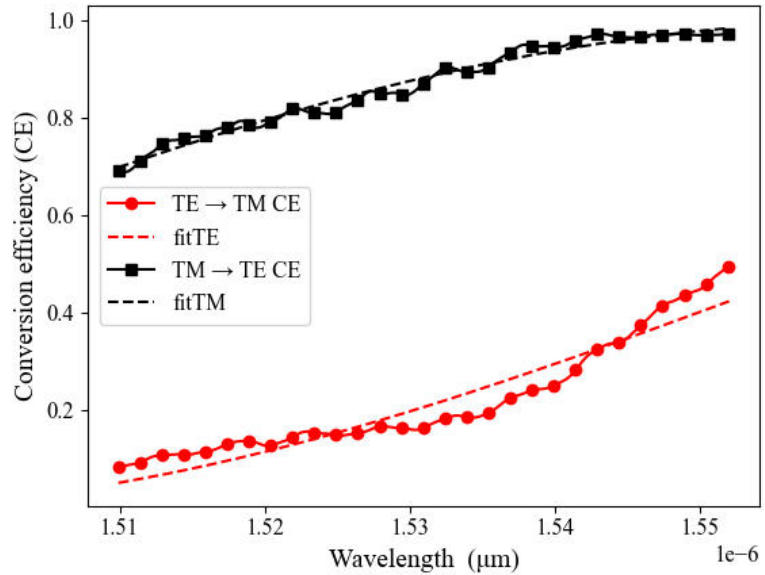


Figure 27.17: TE generator conversion efficiency for the converter length of 66.7 μm and widths of 1.425 and the bimodal section length of 46.5 μm.

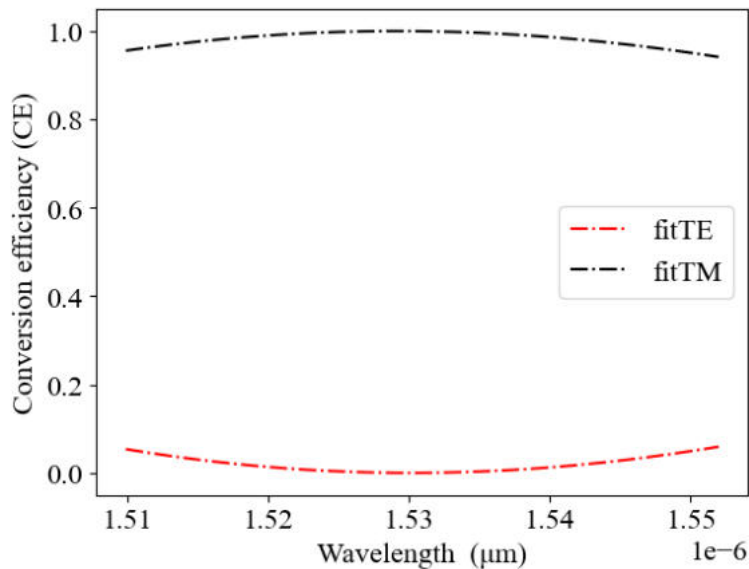


Figure 27.18: TE generator conversion efficiency for the converter length of 66.7 μm and widths of 1.425 and the bimodal section length of 46.5 μm .

27.3.1 Polarization independent semiconductor optical amplifier⁵

For SOAs to operate in a fibre optic network, polarization independence is a prerequisite. Since SOAs are planar devices, often making use of quantum wells or quantum dots as an active medium, TE and TM polarized light usually experience different gains. Furthermore, the use of SOAs in switches and wavelength converters is compromised, since the phase shift and the non-linear response are also polarization dependent. In order to obtain a low polarization dependent gain (PDG), a number of different approaches have been followed. The most common way to reduce PDG is to apply a specific amount of strain to the materials [408]. In this way a PDG in the range of 0.3 to 1 dB has been obtained. This technique can however be difficult, and in some cases even impossible, to apply [409]. It also frequently results in compromises with respect to optimal performance parameters of the SOA, since one degree of freedom in the design has to be sacrificed. Furthermore the effective index, and consequently the phase transfer and the non-linear response, are not independent of polarization (see, e.g., [410]). An alternative method is the use of on-chip polarization handling. In [411] a device is presented which uses an averaging solution. The polarization is converted halfway between two SOA sections and hence the polarization properties are averaged out over the two polarization states. This approach avoids the disadvantages of the strain compensation technique mentioned above. Using a PC not only eliminates the PDG, it also compensates polarization effects in phase shift and non-linear effects (like SPM or XPM). This compensation is obtained without limiting the design options for the SOA.

*polarization
dependent gain*

Principle of polarization independent SOA

A polarization independent SOA can be obtained by placing a passive PC between two identical SOA sections. Suppose that a TE polarized mode with power P_{in} is injected in

⁵This section is based on a paper from Manuela Felicetti [407].

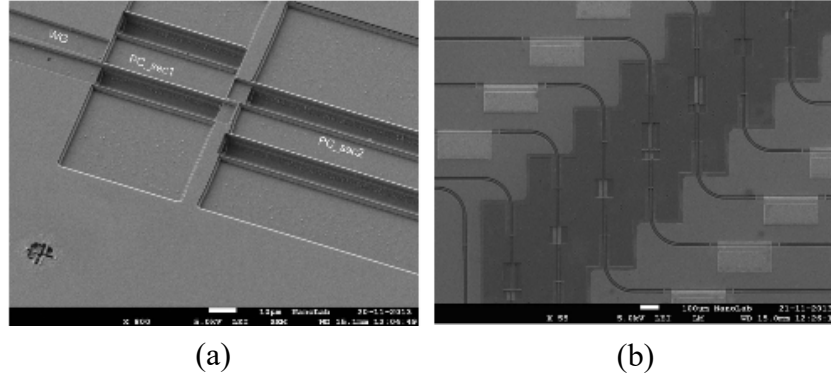


Figure 27.19: SEM-pictures of realized PI-SOA. (a) Two-section polarization converter. (b) SOA-sections with added PCs.

the circuit; if the PC gives a full conversion ($C = 1$) from TE to TM and vice versa, the output power P_{out} is:

$$P_{out} = G_{TM}G_{TE}P_{in} \quad (27.13)$$

with G_{TE} and G_{TM} the gain of the SOA in the TE and TM case, respectively. If a TM polarized mode is injected at the input of the circuit, the output power is:

$$P_{out} = G_{TE}G_{TM}P_{in} \quad (27.14)$$

Thus, by using a full conversion PC, the circuit gives a signal amplification independent of the input polarization (i.e., assuming that the SOAs are equal and not in saturation). If $C < 1$, the output power is:

$$P_{out,TE} = C \cdot G_{TM}G_{TE}P_{in} + (1 - C)G_{TE}^2P_{in} \quad (27.15)$$

if the input mode is TE. For TM input the output power is:

$$P_{out,TM} = C \cdot G_{TE}G_{TM}P_{in} + (1 - C)G_{TM}^2P_{in} \quad (27.16)$$

Thus, in this case, the output power depends on the input polarization and an estimate of C can be obtained from measuring the PDG. A chip containing several Polarization Independent SOA (PI-SOA) structures, but still without the PC, was designed and fabricated within an InP multi-project wafer (MPW) run [412]. An unprocessed space of $500\mu\text{m}$ is left in order to fabricate the PC afterwards, together with connecting waveguides [see Fig. 27.19]. The SOA is based on a single mode weak waveguide. This weak waveguide is obtained using a wet etch-stop scheme, hence the process depends on the crystal orientation. The weak waveguide and the SOA need to be defined in the $[-110]$ direction, in order to obtain straight sidewalls [160]. The sloped sidewall of the PC is also obtained with a wet etch, and requires the PC to be defined in the $[110]$ direction.

Experimental results

The characterization of the integrated polarization converters is done by measuring the polarization dependence of the transmission through the PI-SOA circuits as a function of wavelength and SOA current. Figure 27.20(a) shows that the PDG is reduced

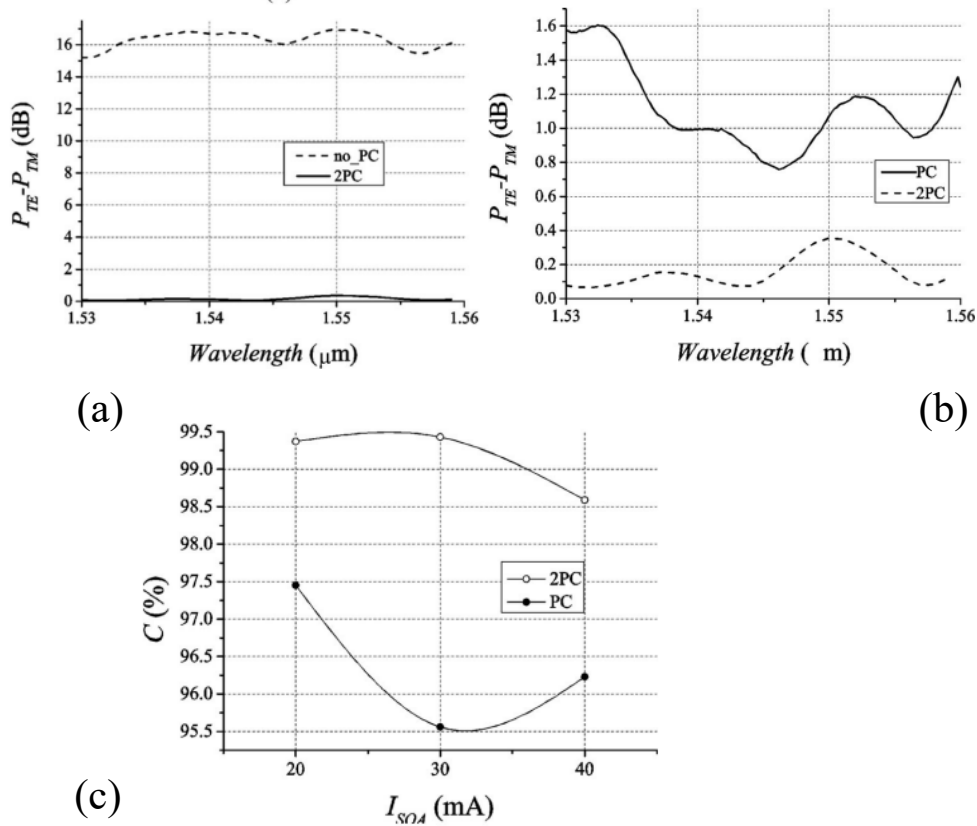


Figure 27.20: (a) PDG of a SOA and a PI-SOA. (b) PDG of two PI-SOAs, with a single section PC and with a two-section PC. (c) Polarization conversion minima for single and double section PCs.

dramatically when the PC is placed halfway between two SOA sections; $P_{TE}-P_{TM}$ for $\lambda = 1.55 \mu\text{m}$ decreases from 17 dB to only 0.35 dB.

Fig. 27.20(b) shows $P_{TE}-P_{TM}$ as a function of the wavelength for two PI-SOA devices (300 μm long SOAs, 30 mA injected current): one with a double section PC (indicated with “2PC”) and the other with a single section PC (indicated with “PC”). Even though both devices show a low PDG, the double section converter has a much improved performance with a PDG below 0.4 dB over the C-band. In Fig. 27.20(c) the PC conversion efficiency C , averaged over the C-band, is shown. This is derived from the measurement results, assuming that both SOA sections are perfectly identical. Of course the value of C cannot depend on the SOA current, so the fact that the derived value nevertheless varies with different current settings indicates that the SOA sections are not exactly equal. Since unequal SOA sections deteriorate the PDG this implies that the estimate for C is a lower boundary. Thus the polarization conversion must be above 99.5% in the case of the double section PC, while it is above 97.5% for the single section PC. This result confirms the superior performance of the double-section converter. Comparing test structures with and without a double section PC (with 300 μm long SOA sections), an insertion loss below 0.5 dB for the double section PC has been estimated.

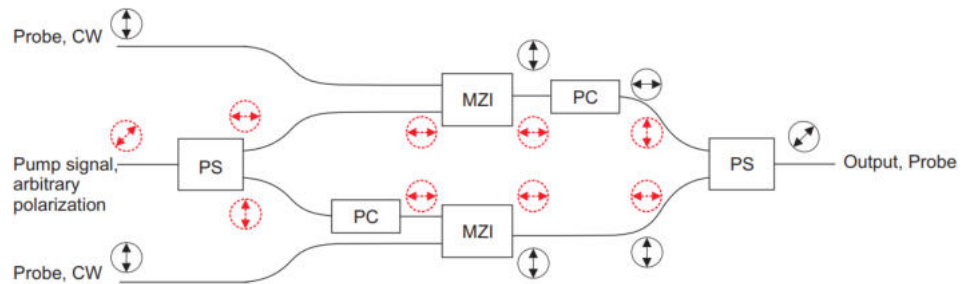


Figure 27.21: POLARIS wavelength converter.

27.3.2 POLARIS (Polarization Labeling for Rejection and Isolation of Signals)⁶

wavelength
converter

In this section the capability of polarization handling is demonstrated by the application of polarization diversity in a wavelength converter (WLC). The polarization is used to add functionality. The polarization is very stable inside a PIC and is not easily transferred from one polarization into the other. The polarization can thus be used to label signals, and by making use of this, select and filter them. This is the principle of POLARIS (Polarization Labelling for Rejection and Isolation of Signals). It is a polarization diversity scheme in which the polarization is used to identify signals. It allows filter-free, co-propagation wavelength conversion and conversion to the same wavelength. As an additional advantage POLARIS allows polarization independent operation. This section will first explain the concept of POLARIS as applied to a wavelength converter (WLC) and an all optical switch. The concept is investigated with a simulation study.

Principle of the POLARIS wavelength converter

The POLARIS concept can be applied for devices in which two optical signals interact and have to be separated at the output. The basic idea is to give both signals, the pump and the probe signal, well defined, but orthogonal polarizations. The polarization thus is a label for the signals and can be used for filtering. A number of different configurations are possible as will be explained in this section. POLARIS has the additional advantage that it can be made polarization insensitive (even when using polarization sensitive SOAs) for one of the signals. The basic principle, applied to a wavelength converter, will be explained first. Fig. 21 shows the schematic configuration of the POLARIS wavelength converter. In the WLC case, the assumption is made that the probe signal, which is locally generated, has a fixed and stable polarization, whereas the pump signal, coming from the fibre-network, has an arbitrary (and varying) polarization.

In the figure the arrows give an indication of the state of polarization of the signals in the device. TE polarized light is indicated as horizontal, TM as vertical. The pump signal is indicated by the dashed circles, the probe by the solid circles. The signal from the network (pump signal) arrives in an unknown polarization state. This signal is split into two orthogonal polarizations in the input polarization splitter (PS). In the lower branch, the polarization is rotated in the polarization converter (PC) to have the pump signal in both branches in the same polarization (TE). These signals are injected into the MZIs together with the locally generated CW light (probe signal) in the orthogonal

⁶This section has been partially copied from the PhD Thesis from Luc Augustin [161], Chapter 7.

polarization (TM). After interacting in the MZI the signal information is transferred to the probe wavelength and both signals have to be separated. This is done by rotating the polarization of the upper branch and then using a polarization splitter/combiner to combine the (probe) signals from both branches. As only TE in the upper and TM in the lower input of the combiner will couple to the output, filtering of the unwanted remains of the pump signal occurs. Note that this is not an interferometric coupling; hence the phase difference between the signals will not be important. It will influence the state of polarization of the output light, but not the amplitude.

If the polarization converters are not perfect, the small unconverted part of the probe in the upper branch can interfere in the output polarization splitter if this splitter is also imperfect. The same will happen for the pump signal, here the influence is even smaller as this signal is filtered twice, first at the input, and at the output. In both cases it is a very small fraction which will not cause problems for most applications.

Simulation study and POLARIS concepts

The POLARIS concept is studied by simulations using a commercial circuit simulator [413]. The performance of the device is investigated to obtain the window of operation for different parameters of the components. The polarization components used in the simulations are assumed to have efficiencies (conversion and splitting) of 95% or 99%, and excess losses of 2 dB. The SOA is modelled using a length-averaged rate-equations model. The effective α -factor of the SOA is a parameter in the simulation. In the simulations values of 5 and 8 are used. ASE is added as white noise to the output of the SOA. The SOA is wavelength and polarization independent. The SOA-model can be extended by placing a polarization dependent attenuator in front of the SOA, this will mimic polarization-dependent gain. In the POLARIS concept the polarization definition at the input of the SOA is fixed and therefore no significant influence is expected from polarization dependence of the SOA. The probe has a power of -8 dBm in each branch, and is TM polarized. For the pump signal, the power and polarization are varied. The pump signal is modulated with a 10 Gb/s PRBS data signal with an Extinction Ratio of 7 dB. The basic POLARIS design (as shown in Fig. 27.21) is investigated when it consists of well performing components: SOAs with an α -factor of 8, and polarization components with 99% efficiency. The Bit Error Rate (BER) as function of the input power for different polarizations is plotted in Fig. 27.22. There is a large input power range of 15 dB for which the BER is well below 10^{-12} for all polarizations. The small difference between the polarizations is explained by the different losses for the different paths. For TE polarized pump light (0°), 99% of the light is coupled to the upper POLARIS branch. No additional losses are present in this path, so almost all the power reaches the SOA. Thus for TE the lowest input power is required. For TM polarized pump light (90°), 99% of the light is coupled to the lower branch, here a PC is present with 2 dB loss, hence the BER curve is shifted to 2 dB higher input powers. For 45° , the worst case, the pump light is split equally into the 2 branches, so 3 dB more power is needed to compensate for this. Furthermore, the TM part has an additional 2 dB loss. This explains the shift with respect to TE. Apart from the BER, the Extinction Ratio (ER) and the filtering of the pump is investigated. The filtering of the pump is expressed as the isolation, defined as the ratio between the probe and pump signal at the output of the device. In Fig. 27.23 the results are given for all three quantities. A comparison is made between the use of a polarization-independent SOA and a polarization-dependent SOA. In the latter, the TM gain is 3 dB lower, and the probe signal is increased by 3 dB to compensate for this. These simulations were performed for the worst case: a polarization of 45° for the pump signal.

*alpha
-factor@ α -factor*

Bit Error Rate

*extinction ratio
isolation*

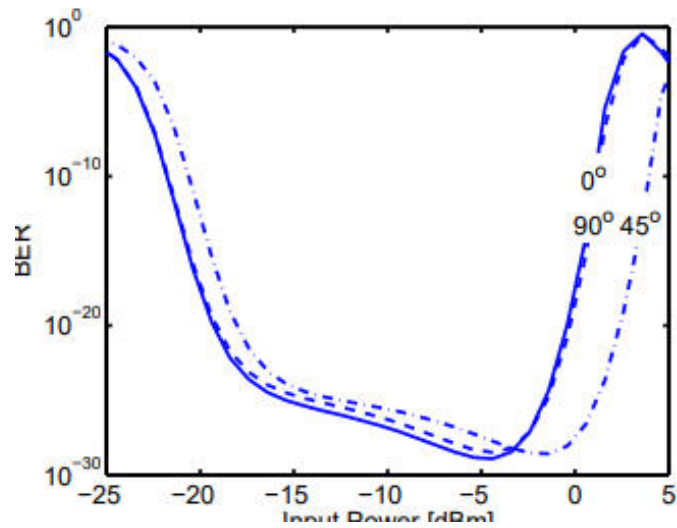


Figure 27.22: BER simulation for POLARIS, 99% efficient polarization components, polarization independent SOA with $\alpha = 8$, changing polarization.

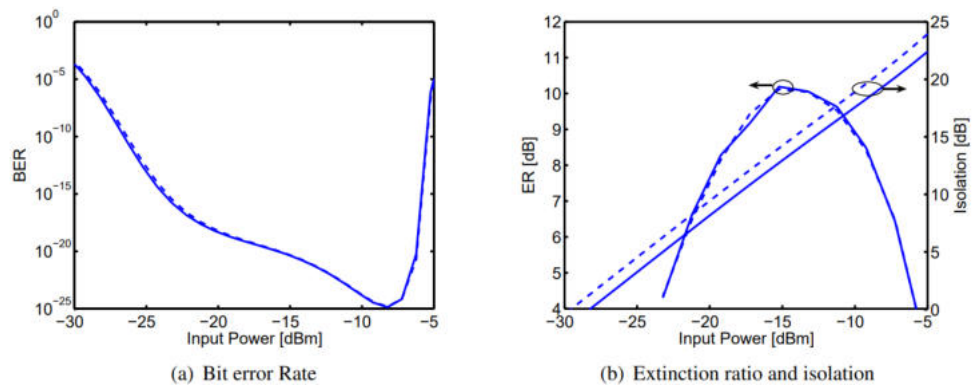


Figure 27.23: Simulation results for POLARIS, 99% efficient polarization components, solid lines for a polarization independent SOA, dashed lines for a polarization dependent (TM gain 3 dB lower) SOA.

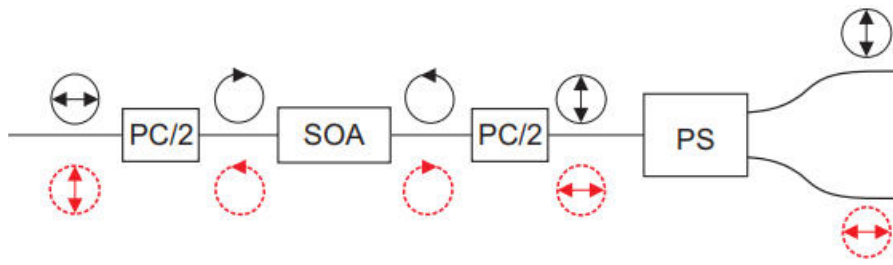


Figure 27.24: Integrated polarization MZI optical switch.

The results indicate that the use of a polarization-dependent SOA does not have a large influence on the performance. The largest difference is in the isolation. This is 1.5 dB higher for the polarization dependent SOA, because the unwanted TM fraction of the pump is less amplified. In the power range from -20.5 dBm to -7.5 dBm the BER is lower than 10^{-12} , and the ER is above 7 dB, so there is regeneration. If an isolation of more than 20 dB is desired, this can only be achieved for powers of -7.5 dBm (or higher).

27.3.3 Polarization MZI optical switch

Polarization can be used to provide light with two independent virtual paths in the same physical waveguide. This can be applied to form an MZI. In a traditional MZI, two different physical paths are used; the phase difference between the two paths results in an interference at the output coupler. The polarization switch (Fig. 27.24) is basically an MZI in which the two arms are separated by using different polarizations. Nonlinear polarization rotation in an SOA can be used for switching and wavelength conversion [414],[415]. An integrated version of this component is possible with the polarization handling devices introduced here. The advantage is a smaller footprint and lower losses, because of the avoidance of bends. At the input of the switch, the pump and the probe are converted to orthogonally circular polarized signals in the input half-PC. Both signals are injected into the SOA which functions as a nonlinear phase shifter. At the output of the SOA, the TE and TM polarized parts of the signals have experienced a power-dependent phase shift. The signals are combined again into the output half-PC. Depending on this relative phase shift, the probe couples to TE or TM. By putting a polarization splitter at the output, switching can be obtained.

27.3.4 Polarization switchable laser

The polarization MZI can also be used to achieve polarization control at the output of a PIC. The integration of a laser with a polarization switch is depicted in Fig. 27.25. The integration of the laser depends on the application; it can be a simple Fabry-Perot laser, a short integrated DBR laser [416] or a multi-wavelength laser [417]. The functioning of the device is the same as in the previous section, as can be seen in the Poincaré sphere of Fig. 27.26. The laser has a fixed and stable output polarization, normally TE (E_1 in Fig. 27.26). The first half PC converts the polarization to a circular polarization (E_2). The phase modulator determines the eventual output polarization. The output PC converts the signal back to a linear polarization. If both PCs are the same, a phase shift of π will result in TE output polarization (E_4), zero (or 2π) phase shift will result in TM. Any other phase shift results in a linear SOP with a controllable angle of polarization.

Poincaré sphere

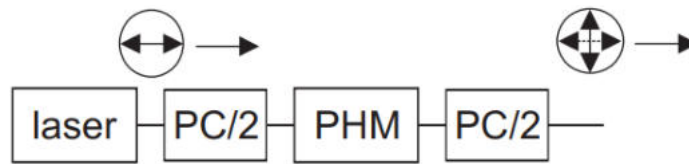


Figure 27.25: Schematic of the laser with switchable polarization.

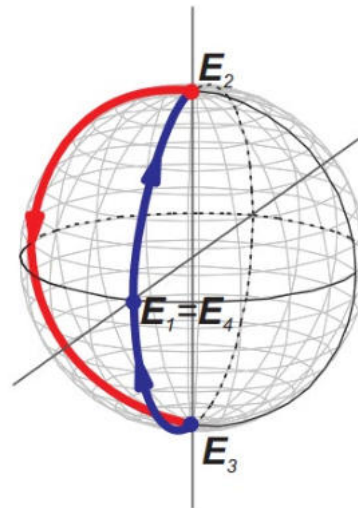


Figure 27.26: Poincaré sphere indicating the SOP in the polarization switchable laser.

27.3.5 Polarization control

Several solutions for polarization dependence of PICs are proposed. One of the solutions is a POLARIS scheme for the all-optical switch as depicted in Fig. 27.21. In this schematic the pump polarization should have equal power in TE and TM. A circuit shown in Fig. 27.27 can change an arbitrary state of the polarization (SOP) of the incoming light to achieve this. On the Poincaré sphere in Fig. 28 the relevant manipulations of the SOP are illustrated. A signal with an arbitrary polarization (E_1 in Fig. 27.28) is fed into the circuit. The phase modulator equalizes the phase to obtain a linear polarization E_2 (SOP at the equator of the Poincaré sphere). The half polarization converter equalizes the amplitudes of both polarizations (E_3 at the meridian in the S_2S_3 -plane). The resulting polarization has equal power in both polarizations but an arbitrary phase between them. The MMI at the output of the PC is a 90/10 MMI, by which 90% of the light is led to the output. The other part of the light is led to the PS. At the outputs of the PS (PDs) measure the intensity of the light in each polarization. This information can be fed back to control the phase modulator at the input. This circuit allows conversion from an arbitrary SOP to a SOP with equal power in both polarizations.

This concept can be extended to convert an arbitrary polarization at the input to the desired polarization at the PIC. As usually TE polarization is preferred, because of its higher gain. A circuit is presented in which any SOP is converted to TE. The schematic is shown in Fig. 27.29. The SOPs are visualized on the Poincaré sphere in Fig. 27.30.

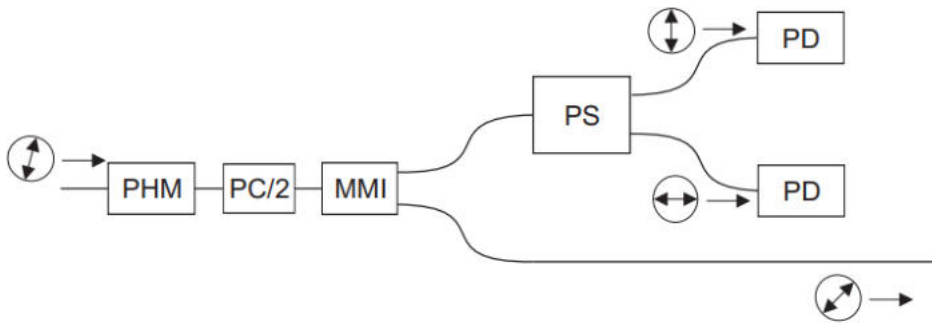


Figure 27.27: Schematic of the 50-50 polarization controller.

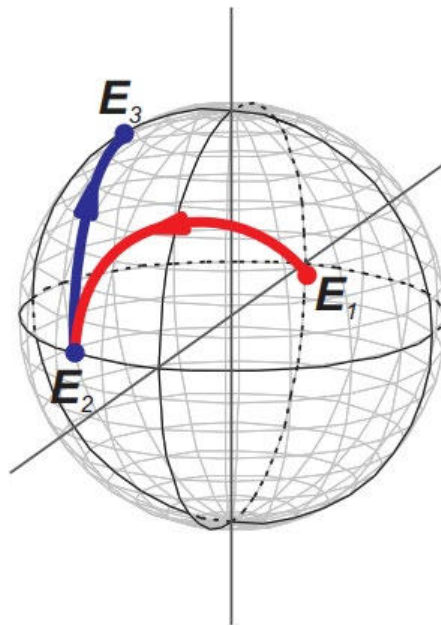


Figure 27.28: Poincaré sphere indicating the SOP in the polarization controller.

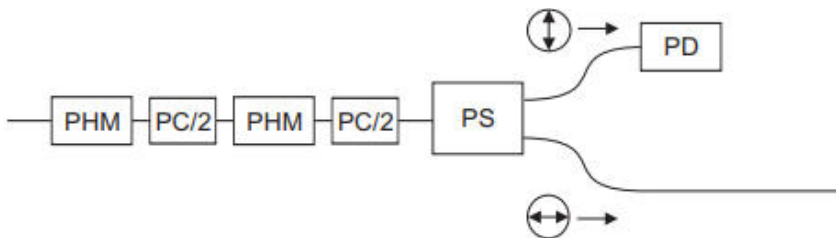


Figure 27.29: Schematic of the polarization controller.

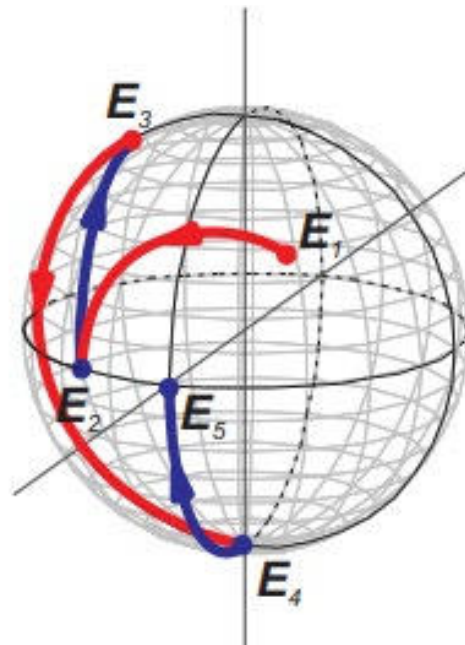


Figure 27.30: Poincaré sphere indicating the SOP in the polarization controller.